



# Amyloid-beta impairs TOM1-mediated IL-1R1 signaling

Alessandra Cadete Martini<sup>a</sup>, Angela Gomez-Arboledas<sup>b</sup>, Stefania Forner<sup>a</sup>, Carlos J. Rodriguez-Ortiz<sup>c</sup>, Amanda McQuade<sup>a,d,e</sup>, Emma Danhash<sup>a,d,e</sup>, Jimmy Phan<sup>a</sup>, Dominic Javonillo<sup>a</sup>, Jordan-Vu Ha<sup>a</sup>, Melanie Tram<sup>a</sup>, Laura Trujillo-Estrada<sup>a,b</sup>, Celia da Cunha<sup>a</sup>, Rahasson R. Ager<sup>a</sup>, Jose C. Davila<sup>b</sup>, Masashi Kitazawa<sup>c</sup>, Mathew Blurton-Jones<sup>a,d,e</sup>, Antonia Gutierrez<sup>b</sup>, David Baglietto-Vargas<sup>a,b,d,1</sup>, Rodrigo Medeiros<sup>a,f,1</sup>, and Frank M. LaFerla<sup>a,d,1</sup>

<sup>a</sup>Institute for Memory Impairments and Neurological Disorders, University of California, Irvine, CA 92697; <sup>b</sup>Department of Cell Biology, Genetics and Physiology, Faculty of Sciences, Instituto de Investigación Biomédica de Málaga-IBIMA, Network Center for Biomedical Research in Neurodegenerative Diseases (CIBERNED), University of Málaga, Málaga 29010, Spain; <sup>c</sup>Center for Occupational and Environmental Health, School of Medicine, University of California, Irvine, CA 92697; <sup>d</sup>Department of Neurobiology and Behavior, University of California, Irvine, CA 92697; <sup>e</sup>Sue and Bill Gross Stem Cell Research Center, University of California, Irvine, CA 92697; and <sup>f</sup>Clem Jones Centre for Ageing Dementia Research, Queensland Brain Institute, The University of Queensland, Brisbane, QLD 4072, Australia

Edited by David M. Holtzman, Washington University School of Medicine, St. Louis, MO, and accepted by Editorial Board Member Carl F. Nathan September 5, 2019 (received for review August 19, 2019)

**Defects in interleukin-1 $\beta$  (IL-1 $\beta$ )–mediated cellular responses contribute to Alzheimer’s disease (AD). To decipher the mechanism associated with its pathogenesis, we investigated the molecular events associated with the termination of IL-1 $\beta$  inflammatory responses by focusing on the role played by the target of Myb1 (TOM1), a negative regulator of the interleukin-1 $\beta$  receptor-1 (IL-1R1). We first show that TOM1 steady-state levels are reduced in human AD hippocampi and in the brain of an AD mouse model versus respective controls. Experimentally reducing TOM1 affected microglia activity, substantially increased amyloid-beta levels, and impaired cognition, whereas enhancing its levels was therapeutic. These data show that reparation of the TOM1-signaling pathway represents a therapeutic target for brain inflammatory disorders such as AD. A better understanding of the age-related changes in the immune system will allow us to craft therapies to limit detrimental aspects of inflammation, with the broader purpose of sharply reducing the number of people afflicted by AD.**

target of Myb1 | TOM1 | IL-1R1 | Alzheimer’s disease | 3xTg-AD

Immune responses need to be tightly regulated in terms of intensity, class, and duration to prevent molecular and cellular damage. While in young healthy individuals inflammation is self-limited, disturbances in the immune system of older subjects may result in a state of low-grade chronic inflammation (1, 2). In the brain, such processes have been implicated with a variable degree of importance in almost all age-related neurodegenerative disorders including Alzheimer’s disease (AD) (3, 4). The endosomal system, known principally for its role in the uptake of molecules from the plasma membrane and surrounding environment, is increasingly being recognized as a critical component in the regulation of inflammatory responses (5, 6). For example, trafficking and sorting of proinflammatory receptors, for which the final destination is the degradation in lysosomes, are known to play an important role in the down-regulation of signaling following ligand stimulation (7–9).

Among numerous inflammatory pathways, the interleukin-1 $\beta$  (IL-1 $\beta$ )–signaling pathway plays a critical pathogenic role in AD (10–12). IL-1 $\beta$  is up-regulated in the brain, cerebrospinal fluid, and plasma of AD patients, directly affecting pathology development (13–15). Previous data indicate that the initial increase in IL-1 $\beta$  levels is associated with the buildup of intracellular A $\beta$  and occurs prior to any apparent glia activation in young 3xTg-AD mice, suggesting an association between both events in neurons (10, 16). A major site of expression of IL-1 $\beta$  and its receptor, interleukin-1 receptor-1 (IL1-R1), is the hippocampus, implicating their potential role in modulating hippocampal memory function. Elevated levels of this cytokine in the brain have deleterious effects on consolidation of spatial memory and in hippocampus-dependent contextual tasks (11, 17). IL-1 $\beta$  impairs long-term potentiation

(LTP) in synaptosomes and, due to a reconfiguration in the IL-1 receptor subunit AcP, aged hippocampal synapses become more sensitive to this cytokine (18). Additional proposed mechanisms for the impairment evoked by IL-1 $\beta$  in the aging brain may involve the activation of mitogen-activated protein kinases (19–21) and brain-derived neurotrophic factor (BDNF), since the consolidation of hippocampus-dependent memory, and associated forms of synaptic plasticity, are dependent upon this molecule (22).

Once bound by IL-1 $\beta$ , IL-1R1 binds to target of Myb1 (TOM1) and is internalized to endosomes to ensure proper resolution of the inflammatory response (23–26). TOM1 is predominantly present in the cytosol and interacts with proteins such as clathrin and toll-interacting protein (Tollip) to regulate endosomal trafficking and lysosomal degradation of ubiquitinated proteins (23, 27). Given that defects in intracellular protein

## Significance

**As we age, the innate immune system becomes dysregulated and is characterized by persistent inflammatory responses, and the chronic inflammation mediated by inflammatory receptors represents a key mechanism by which amyloid-beta (A $\beta$ ) drives the development of cognitive decline in Alzheimer’s disease (AD). A crucial aspect of this process is a failure to resolve inflammation, which involves the suppression of inflammatory cell influx and the endocytosis of inflammatory receptors. We found that ablation of the endosomal adaptor target of Myb1 (TOM1) worsens neuroinflammation, impairs microglial phagocytosis, and significantly exacerbates amyloid deposition. Conversely, restoration of TOM1 reverses these effects and reduces A $\beta$  pathology. These results highlight the importance of endosomal adaptors and their interaction with inflammatory receptors in the pathogenesis of AD.**

Author contributions: M.K., M.B.-J., and A.G. acquired funding; D.B.-V., R.M., and F.M.L. acquired funding and provided supervision; A.C.M., A.G.-A., S.F., R.M., and F.M.L. designed research; A.C.M., A.G.-A., S.F., C.J.R.-O., A.M., E.D., J.P., D.J., J.-V.H., M.T., L.T.-E., C.d.C., R.R.A., and J.C.D. performed research; M.K., M.B.-J., and A.G. contributed new reagents/analytic tools; A.C.M., A.G.-A., S.F., C.J.R.-O., A.M., E.D., J.P., D.J., J.-V.H., M.T., L.T.-E., C.d.C., R.R.A., J.C.D., M.K., M.B.-J., and D.B.-V. analyzed data; and A.C.M., A.G.-A., S.F., C.J.R.-O., L.T.-E., R.R.A., J.C.D., A.G., D.B.-V., R.M., and F.M.L. wrote the paper;

The authors declare no competing interest.

This article is a PNAS Direct Submission. D.M.H. is a guest editor invited by the Editorial Board.

This open access article is distributed under [Creative Commons Attribution-NonCommercial-NoDerivatives License 4.0 \(CC BY-NC-ND\)](https://creativecommons.org/licenses/by-nc-nd/4.0/).

<sup>1</sup>To whom correspondence may be addressed. Email: [d.baglietto@uci.edu](mailto:d.baglietto@uci.edu), [rodrigo.medeiros@neurula.org](mailto:rodrigo.medeiros@neurula.org), or [laferla@uci.edu](mailto:laferla@uci.edu).

This article contains supporting information online at [www.pnas.org/lookup/suppl/doi:10.1073/pnas.1914088116/-DCSupplemental](https://www.pnas.org/lookup/suppl/doi:10.1073/pnas.1914088116/-DCSupplemental).

First published September 30, 2019.

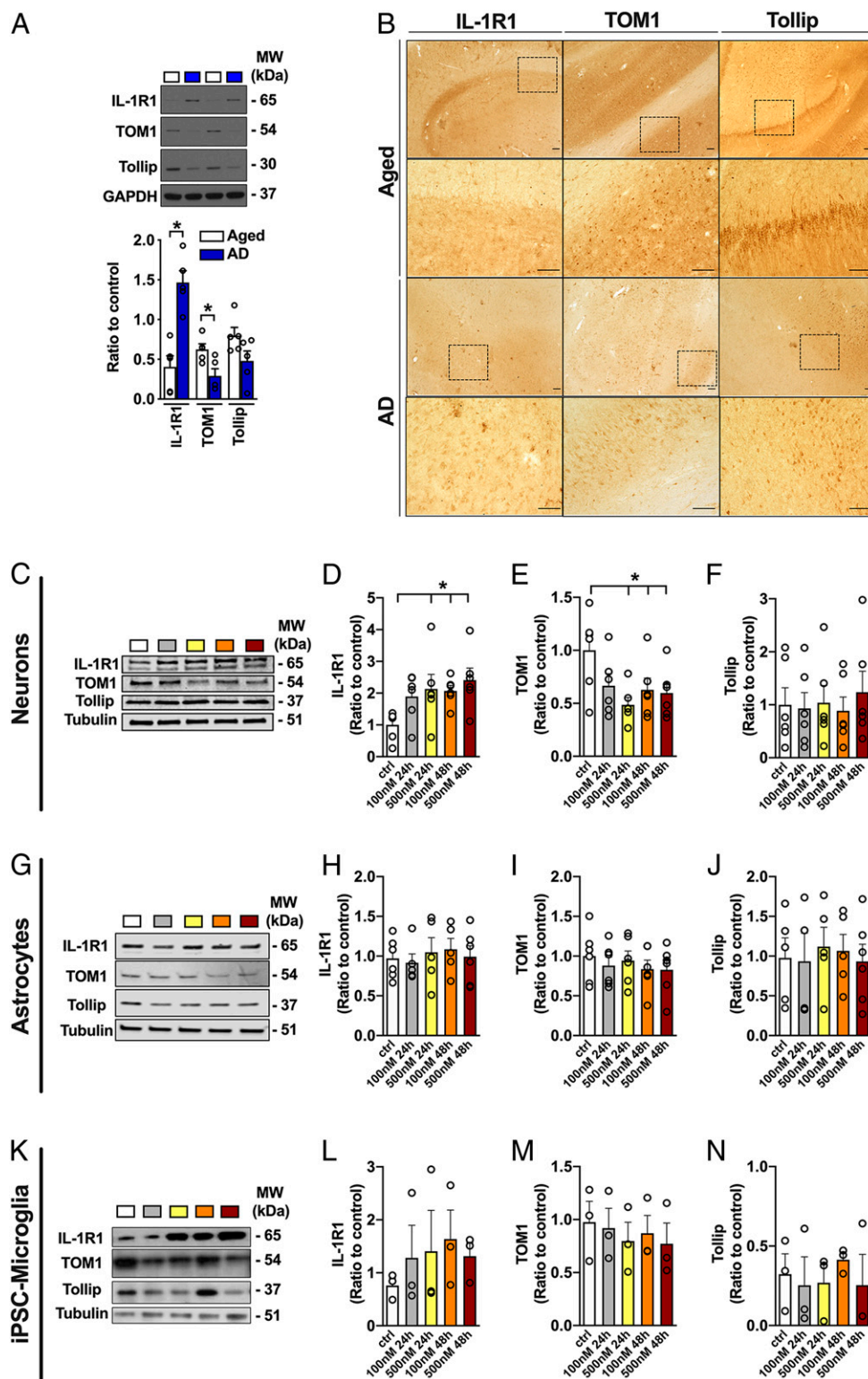


**Fig. 1.** Reduced TOM1 levels are found in AD brains and in neuronal cell culture in the presence of ADDLs. Representative Western blots and quantification show increased IL-1R1 and reduced TOM1 levels in the hippocampus of AD patients (A). Immunohistochemistry staining for TOM1 in AD and age-matched controls (Scale bars, 250  $\mu$ m.) (B). Representative Western blots (C, G, and K) and quantification show increased IL-1R1 (D), decreased TOM1 (E), and unchanged Tollip (F) levels in primary mouse neuronal cell culture after incubation with ADDLs. No significant changes were observed in the levels of IL-1R1, TOM1, or Tollip in astrocytes (G–J) or iPSC-derived human microglia (K–N) in response to ADDLs. Data are represented as mean  $\pm$  SEM. ANOVA, \* $P \leq 0.05$ ,  $n = 3–8$  per group.

clearance (e.g., autophagy and ubiquitin-proteasome system) and trafficking (e.g., endocytosis) have been implicated in the regulation of IL-1 $\beta$  signaling (24, 28) and AD (29–31), it is plausible that

the disruption of these processes may result in overexpression of proinflammatory receptors leading to exacerbated immune responses and cognitive decline.

It remains an open question whether TOM1 plays a role in IL-1R1 signaling in the pathogenesis of AD. Our findings provide *in vivo* and *in vitro* evidence that reduced TOM1 impairs IL-1R1 neuronal internalization and promotes amyloid plaque deposition. Ablating TOM1 also enhances the overall proinflammatory milieu and promotes detrimental changes in microglial morphology and function. This work identifies a critical role for TOM1 in AD, suggesting that impairments on this pathway could dramatically affect the development and progression of AD.

## Results

**Impairment in TOM1 Levels Causes IL-1R1 Overexpression in AD.** For efficient degradation, the IL-1R1 needs to bind to Tollip and TOM1 in order to be internalized to endosomes (23–25). We found that, while the steady-state levels of Tollip are not altered, the expression of TOM1 is significantly reduced in human AD brains and associated with a corresponding increase in the levels of IL-1R1 (Fig. 1 *A* and *B*). To investigate the potential effects of amyloid-beta ( $A\beta$ ) in this signaling pathway, we treated primary mouse astrocytic and hippocampal neuronal cultures and induced pluripotent stem cell (iPSC)-derived human microglia with  $A\beta$ -derived diffusible ligands 1–42 (ADDLs). We observed that, compared to control, the neuronal level of IL-1R1 was increased with growing concentration and incubation time of ADDLs while Tollip levels were not changed (Fig. 1 *C–F*). Conversely, no significant changes were observed in astrocytes or iPSC-microglia (Fig. 1 *G–N*). In AD transgenic mouse brains, TOM1 reduction was also accompanied by increased IL-1R1 and IL-1 $\beta$  levels (Fig. 2 *A–C* and *SI Appendix, Fig. S2A*). To further investigate this matter, we injected adeno-associated virus (AAV) constructs designed to overexpress (AAV1-CAG-mTOM1-WPRE) or knock down (AAV1-GFP-U6-mTOM1-shRNA) TOM1 in the hippocampus of 9-mo-old 3xTg-AD mice. There was a higher infection of neuronal cells, followed by reduced microglial and no astrocytic viral infection (*SI Appendix, Fig. S1*). By knocking down TOM1, the levels of both IL-1R1 and IL-1 $\beta$  were increased (Fig. 2 *A–C* and *SI Appendix, Fig. S2A*). No changes in other inflammatory receptors—TLR4 and TNFR—were observed, suggesting that TOM1 works specifically with IL-1R1 in AD (*SI Appendix, Fig. S2B*). We have also confirmed the expression of IL-1R1 in hippocampal neuronal and microglial cells, with lower expression detected in astrocytes (*SI Appendix, Fig. S2C*) (32, 33). In the hippocampus of 3xTg-AD mice, the receptor was found in both pre- and postsynaptic terminals, with a higher signal observed in the postsynapse (Fig. 2 *D1* and *D2*). In TOM1-WPRE animals, however, the signal not only was more prominent inside the dendrites, but also was associated with the endoplasmic reticulum, in sharp contrast to the high IL-1R1 signal associated with the membrane in Null-AAV- and TOM1-shRNA-treated mice (Fig. 2*D*). These results indicate that the dysfunction in TOM1-mediated endocytosis and degradation exacerbates the steady-state levels of IL-1R1 in AD.

**Knockdown of TOM1 Exacerbates Immune Response.** Considering the importance of TOM1 in shuttling internalized IL-1R1 to lysosomes for degradation, it is possible that reduced TOM1 levels lead to a state of overactivation of the immune response in the brain. In addition to increased IL-1 $\beta$  levels, TOM1-shRNA increased 2 other proinflammatory cytokines, tumor necrosis factor- $\alpha$  (TNF- $\alpha$ ) and KC-GRO, whereas the overexpression of TOM1 increased interleukin-2, a cytokine involved in the control of inflammation and reduction of AD hallmarks in the APP/PS1 $\Delta$ E9 model (*SI Appendix, Fig. S3 A–D*) (34). We used the NanoString nCounter mouse inflammation gene expression panel to perform expression profiling of RNAs that are altered by the manipulation of TOM1 in 3xTg-AD mouse hippocampus. Of the 253 mRNAs tested, 93 transcripts were significantly changed among different groups (*SI Appendix, Table S2*),

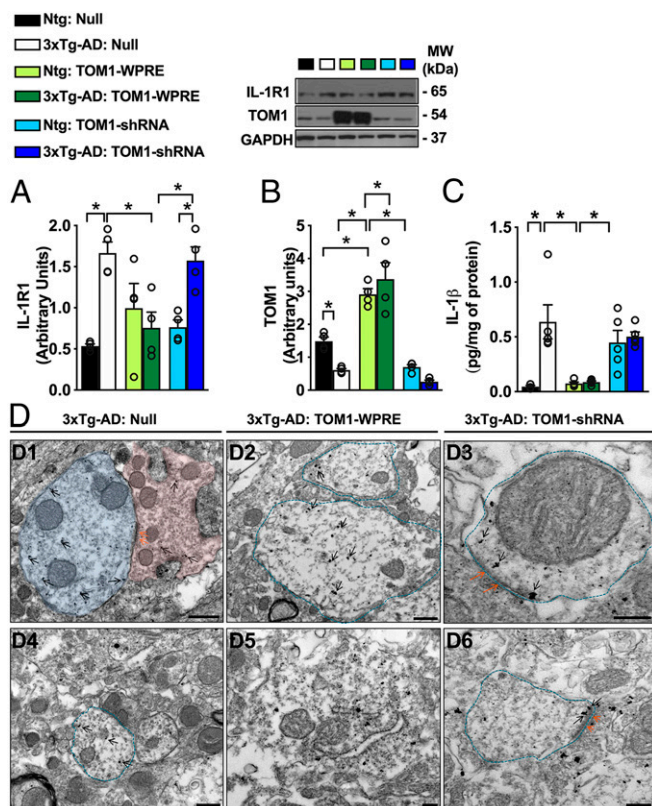


**Fig. 2.** Reduced TOM1 is accompanied by increased IL-1R1 and IL-1 $\beta$  levels. Representative Western blots and quantification show increased IL-1R1 in Null and TOM1-shRNA 3xTg-AD mice (*A*). TOM1 is reduced in Null 3xTg-AD mice, whereas the animals treated with TOM1-WPRE show significantly increased levels of this protein (*B*). IL-1 $\beta$  levels are increased in the hippocampus of 3xTg-AD mice treated with Null and TOM1-shRNA AAVs vs. TOM1-WPRE mice (*C*). Images obtained through electron microscopy reveal the IL-1R1 presence in pre (pink) and postsynaptic (blue) terminals (*D*). In Null (*D1* and *D4*) or TOM1-shRNA-treated mice (*D3* and *D6*), the receptor is expressed closer to the membrane, whereas it appears more internalized and associated with the endoplasmic reticulum on TOM1-WPRE mice (*D2* and *D5*). Black arrows: receptor expression; orange arrows: synapses. (Scale bars: *D1*, *D2*, and *D4*, 0.5  $\mu$ m; *D3*, 200 nm; *D5* and *D6*, 0.2  $\mu$ m.) Data are represented as mean  $\pm$  SEM. ANOVA, \* $P \leq 0.05$ ;  $n = 3–4$  per group.

including genes related to AD onset, chemokines, cytokines, and complement system components. Thus, alterations of genes in specific inflammation-related pathways represent networks altered in response to TOM1 modification.

**Reduced TOM1 Impairs Microglial Phagocytic Efficiency.** The TOM1-shRNA-treated mice presented changes in the glial cell morphology, with a reduction in the total length of processes, the number of branches per microglia cell, and microglial loading (Fig. 3 *A–D*), but no significant changes in the number of Iba1-positive cells in the hippocampus of any of the groups analyzed (Fig. 3*E*). A similar pattern was also seen for astrocytes (Fig. 3 *F–J*). Among other important roles, microglia are the brain's primary cellular agent for clearing extracellular  $A\beta$ , so we quantified the proportion of  $A\beta$  inside microglial phagolysosomes. TOM1-WPRE mice had reduced plaque deposition and increased immunofluorescence intensity and localization of glia within the center of plaques, suggesting that TOM1 deficiency alters the phagocytic activity and the glial response to  $A\beta$  plaques (Fig. 4 *A*, *A1* and *A2*). We further analyzed this response by infecting iPSC-derived human microglia cultures with Lenti open reading frame (ORF) particles, TOM1 (Myc-DDK-tagged), in

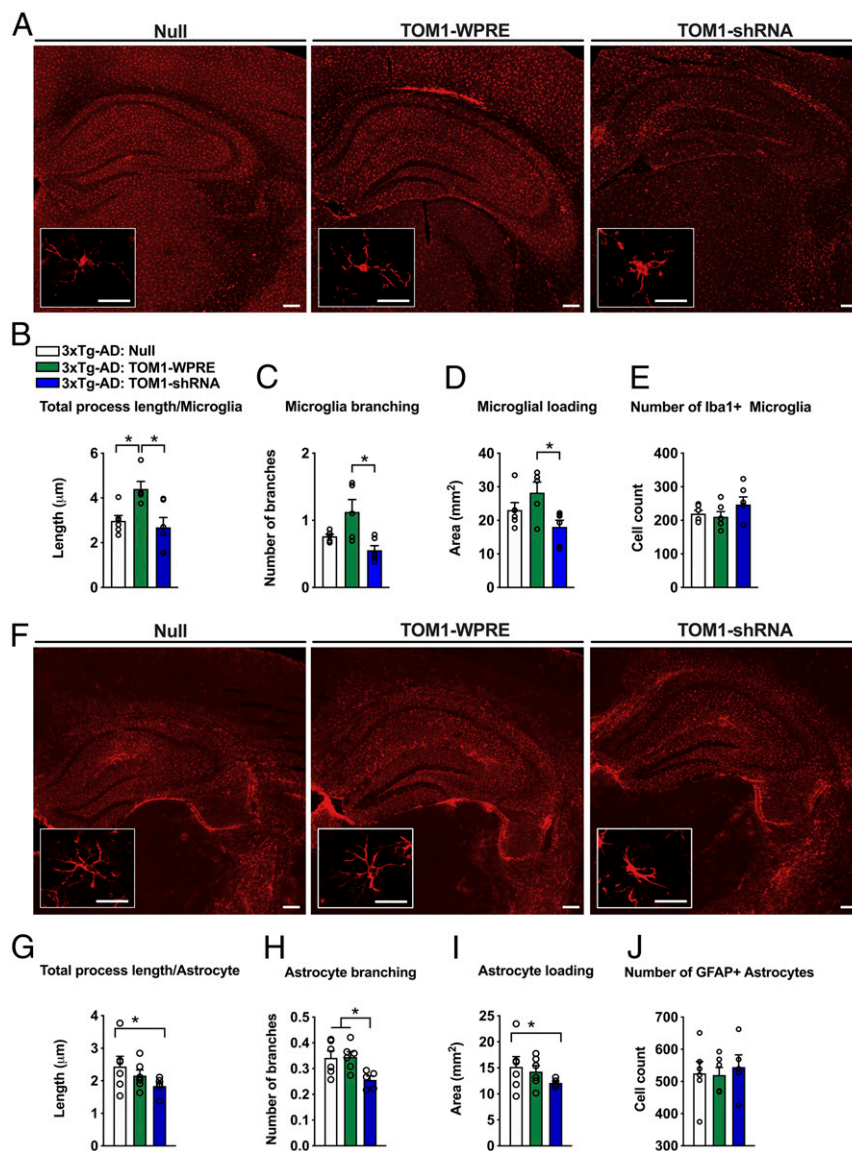


**Fig. 3.** Ablating TOM1 alters glial morphology. (A) Representative images of microglia (Iba1<sup>+</sup>) in the hippocampus of 3xTg-AD mice treated with AAV-Null, AAV-TOM1-WPRE, or AAV-TOM1-shRNA. (Scale bar, 200 μm; *Inset*, 25 μm.) Total process length per microglia (B), the number of branches per microglia (C), and the microglial loading are significantly reduced by TOM1-shRNA (D), while the number of microglia cells does not change (E). Representative images of astrocytes (GFAP<sup>+</sup>) in the hippocampus of 3xTg-AD mice treated with AAV-Null, AAV-TOM1-WPRE, and AAV-TOM1-shRNA (F). (Scale bar, 200 μm; *Inset*, 25 μm.) Total process length per astrocyte (G), the number of branches per astrocyte (H), and the astrocyte loading (I) are significantly reduced by TOM1-shRNA, while the number of astrocytes (J) does not change. Data are represented as mean ± SEM. ANOVA, \**P* ≤ 0.05; *n* = 6 per group.

order to increase TOM1 levels, followed by incubation with fluorescent ADDLs or Aβ fibrils. We then measured the rate of Aβ phagocytosis in a real-time live-imaging system over 24 h. Quantification of bright red fluorescence, indicating cellular uptake of Aβ, revealed significantly increased phagocytosis in TOM1-overexpressing cells (Fig. 4 *B–D*). Compared to the soluble oligomers, Aβ fibrils were phagocytosed at a much faster rate in the presence of increased TOM1.

**Aβ Deposition Is Enhanced by the Reduction in TOM1.** We next addressed whether the manipulation of TOM1 and microglial phagocytosis would impact Aβ pathology in vivo. The TOM1-shRNA mice presented a greater number and area of Aβ plaques (Fig. 4 *E* and *F* and *SI Appendix*, Fig. *S4A*), as well as increased levels of soluble Aβ<sub>38</sub>, Aβ<sub>40</sub>, and Aβ<sub>42</sub> and of insoluble Aβ<sub>40</sub> and Aβ<sub>42</sub> (Fig. 4 *G* and *H*). Interestingly, we found irregular staining

and TOM1 accumulation in proximity to amyloid deposits (*SI Appendix*, Fig. *S4B*). As expected, 3xTg-AD mice presented higher levels of amyloid precursor protein (APP), compared to the nontransgenic (nTg) mice, and increased TOM1 levels led to reduction of β-site APP-cleaving enzyme 1 (BACE1), but not of the other proteins related to the amyloid precursor protein (APP) processing (Fig. 5 *A–E*). The colocalization of TOM1 in dystrophic neurites and neurofibrillary tangles, as well as with proteins from the ubiquitin-proteasome and the autophagy-lysosome systems—2 systems that were first thought to be independent but are actually capable of cross talk—has been reported (35). p62 is an autophagy substrate used as a reporter of autophagy activity, and it delivers ubiquitinated proteins, such as tau, to the proteasome for degradation (36, 37). Increased levels of p62 facilitate the removal of Aβ and tau in the APP/PS1ΔE9 mouse model (38). We found a significant

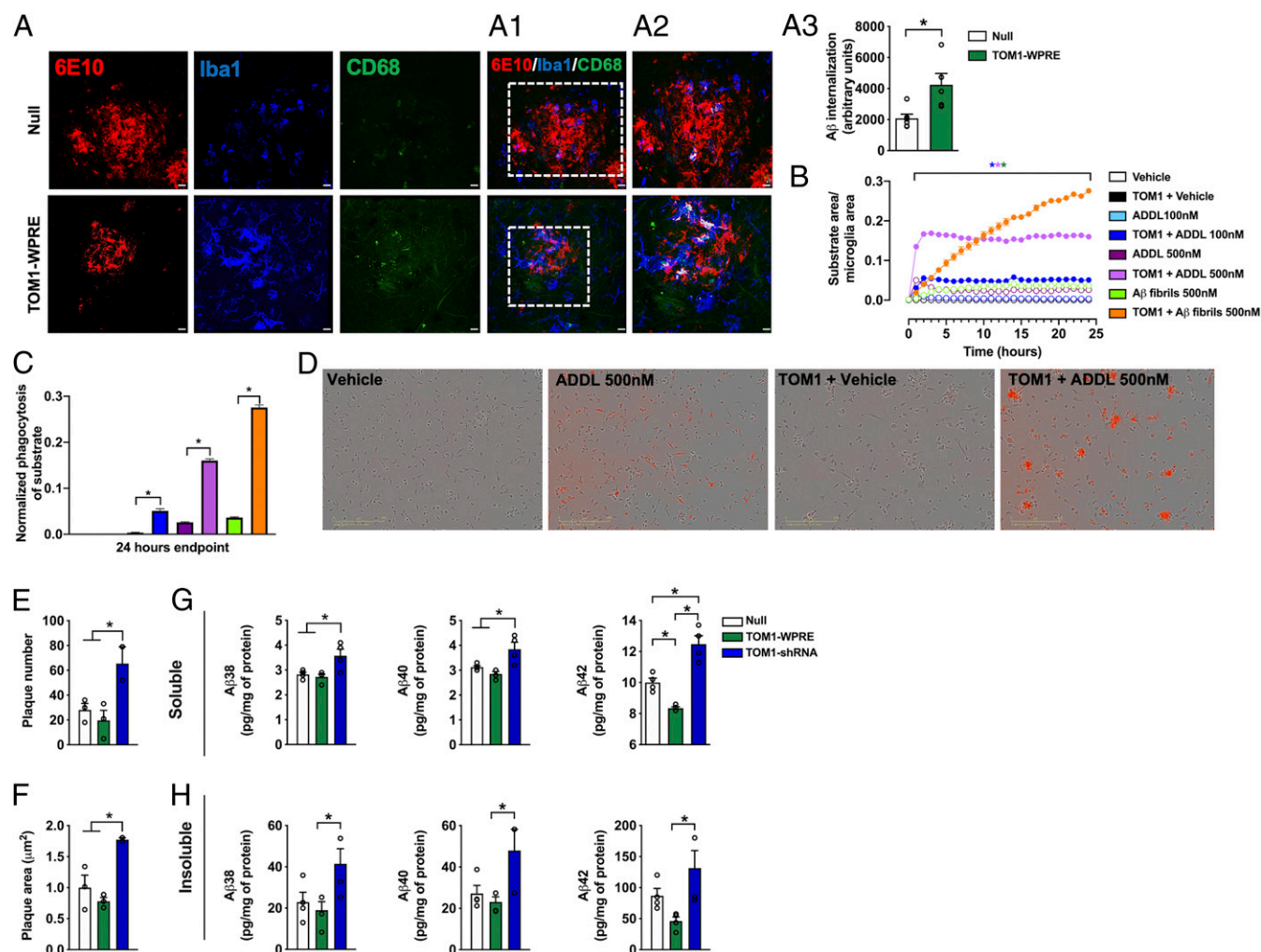


**Fig. 4.** TOM1 ablation reduces A $\beta$  phagocytosis. Representative immunohistochemical images of A $\beta$  plaques (6E10: red), microglia (Iba1: blue), and microglial phagolysosomes (CD68: green) (A, A1, and A2). Three-dimensional reconstruction of Iba1, A $\beta$ , and phagolysosomes inside microglia (A1 and A3). (Scale bars, A and A1: 150  $\mu$ m; A2: 100  $\mu$ m.) Quantification of A $\beta$  within phagolysosomes revealed a significant increase in A $\beta$  internalization in TOM1-WPRE mice (A3). iPSC-derived microglia cells were infected with TOM1 lentivirus and incubated with ADDLs or A $\beta$  fibrils, and the rate of microglia phagocytosis was measured over 24 h in real time. TOM1 infection significantly increased the phagocytosis of 100 and 500 nM, as well as A $\beta$  fibrils (B and C). Representative images of 555-labeled ADDL uptake in iPSC-microglia during live imaging sessions (D). TOM1-shRNA significantly increased the total number (E) and area (F) of A $\beta$  plaques in the hippocampus of 3xTg-AD mice. A $\beta$  V-PLEX immunoassay reveals significant increase in A $\beta$ <sub>38</sub>, A $\beta$ <sub>40</sub>, and A $\beta$ <sub>42</sub> in soluble (G) and insoluble (H) hippocampal lysates from TOM1-shRNA-treated mice. Data are represented as mean  $\pm$  SEM. ANOVA, \* $P$   $\leq$  0.05;  $n$  = 3–4 per group.

increase in p62 levels in TOM1-WPRE mice, but no significant changes in LC3B-II/LC3B-I ratio (Fig. 5 F and G), supporting the idea that changes in TOM1 interfere directly with the microglial ability to remove A $\beta$ . Thus, these protein-degradation systems could be responsible for the dysfunction of TOM1 in the presence of A $\beta$  plaques and, consequently, of IL-1R1 in the AD brain.

**Loss of TOM1 Causes the Exacerbation of Cognitive Decline.** To determine whether TOM1 deficiency affects AD-related cognitive changes in mice, we assessed spatial learning and memory using the Morris water maze. First, we found that changes in TOM1 levels do not impact cognitive function in healthy nTg animals. However, acquisition performance in 3xTg-AD mice treated with TOM1-WPRE was similar to that observed in nTg mice, suggesting that these animals learned the location of the hidden platform more quickly than did AD mice treated with Null-AAV or TOM1-shRNA mice (Fig. 6A). During the test day, TOM1-shRNA-treated 3xTg-AD mice spent less time in the zone of the platform, crossed the platform fewer times, and took longer to

find the hidden platform (Fig. 6 B–D), and these differences were not due to locomotor impairments as demonstrated by distance and speed analyses (Fig. 6 E and F). Moreover, these animals also presented a reduced percentage of freezing behavior in the contextual fear-conditioning test (Fig. 6G), but no changes were seen in the novel object task (Fig. 6H). We have also measured the levels of BDNF and pCREB/CREB, as these are important factors related to learning and memory processes (39–41), but no significant changes were found. Altogether, our studies indicate that TOM1 rescue the cognitive function in AD mice indirectly by changing levels of A $\beta$  and proinflammation, without altering memory-related pathways.

**Tollip Ablation Worsens Cognition without Affecting A $\beta$  Levels.** The induced ubiquitination of IL-1R1 by IL-1 $\beta$  is part of the basis for interaction with Tollip, which is also required for sorting of the receptor for lysosomal degradation. Supportive of this possibility is the observation that the production of the proinflammatory cytokines interleukin-6 and TNF- $\alpha$  was significantly reduced after stimulation with low doses of IL-1 $\beta$  and lipopolysaccharide in

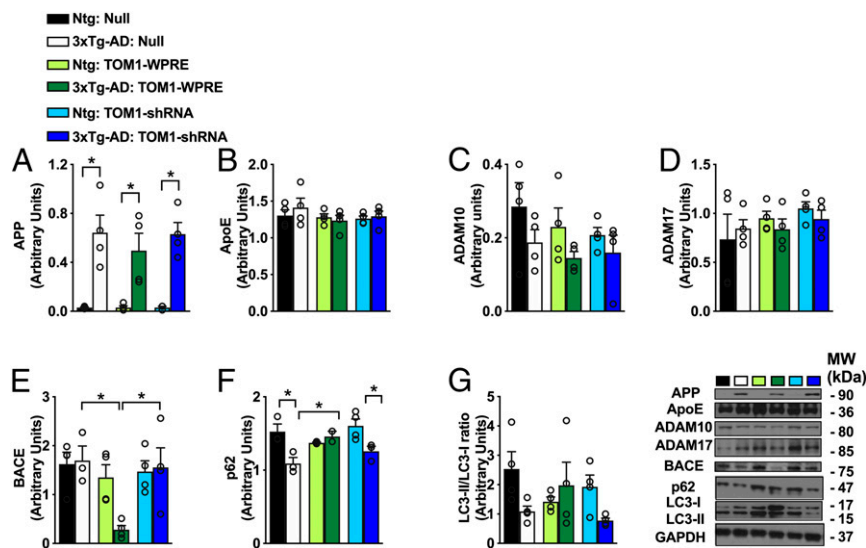


**Fig. 5.** TOM1 overexpression alters BACE1 and p62 levels proteins. Representative Western blots and quantification show increased APP (A) in all 3xTg-AD groups. BACE was reduced in TOM1-WPRE compared to Null and TOM1-shRNA 3xTg-AD mice (E), but no significant changes were found in APOE (B), ADAM10 (C), or ADAM17 (D). Moreover, TOM1 overexpression increased the levels of p62 (F) without changing the LC3-II/I ratio (G). Data are represented as mean  $\pm$  SEM. ANOVA, \* $P \leq 0.05$ ;  $n = 4$  per group.

Tollip knockout mice, suggesting that Tollip may regulate the magnitude of inflammatory cytokine production (24, 28). Accordingly, a different cohort of animals was injected with AAV1-GFP-U6-mTollip-shRNA to knock down Tollip and serve as a means of comparison to the effects promoted by TOM1 manipulation. We found reduced levels of Tollip and increased IL-1R1 in 3xTg-AD-Null-treated mice versus nTg mice, aspects that were exacerbated by the Tollip-shRNA treatment (SI Appendix, Fig. S5A and B). However, levels of IL-1 $\beta$  were not changed with treatment (SI Appendix, Fig. S5C). Similar to TOM1-shRNA-treated mice, animals treated with Tollip-shRNA presented a higher expression of the receptor closer to the cell membrane, as observed through electron microscopy (SI Appendix, Fig. S5D). Knocking down Tollip also modified the morphology of microglia and astrocytes, without changing the number of these cells (SI Appendix, Fig. S5E–N), and increased the area of A $\beta$  plaques (SI Appendix, Fig. S6A) but did not significantly change any of the soluble and insoluble A $\beta$  levels measured (SI Appendix, Fig. S6B–G). As seen with the other treatment groups, Tollip-shRNA-treated mice had higher escape latency during the acquisition phase of the Morris water maze and a reduced number of crosses (SI Appendix, Fig. S6H–M), and the freezing behavior in the contextual fear conditioning test was also reduced in comparison to nTg mice (SI Appendix, Fig. S6N). However, as the ablation of this protein was also detrimental in nTg mice, the involvement of A $\beta$ -independent mechanisms cannot be excluded; however, more studies are necessary to confirm this idea.

## Discussion

The activation of brain immune responses through IL-1R1 signaling is critical for host defense. However, excessive or inappropriate activation because of unrestrained signaling of this receptor is detrimental and has been linked to the pathogenesis of AD (42, 43). Termination of IL-1 $\beta$ -induced inflammatory response requires the activation of TOM1, which inhibits further signaling by targeting IL-1R1 to endosomes for efficient lysosomal degradation (23, 28). The relevance of intracellular protein trafficking in the regulation of IL-1 $\beta$  signaling suggests that dysfunction of endocytosis may result in excessive expression of IL-1R1, which in turn exacerbates inflammatory responses. We found that TOM1 deficiency exacerbates the inflammatory

response and increases A $\beta$  plaque deposition. These data suggest that, even in older animals, restoration of proper receptor internalization can be beneficial and ameliorate cognitive deficits, a finding which has strong therapeutic implications.

Our findings are consistent with the notion that up-regulation of IL-1R1 in the aged hippocampus can potentiate the IL-1 $\beta$  inflammatory response (18). Previous reports have shown that the loss of synaptic connections induced by IL-1 $\beta$  requires both pre- and postsynaptic mechanisms (15), which could explain the detrimental consequences of the increased receptor expression observed in our study. IL-1 $\beta$  can boost its own expression through autocrine actions on microglia and paracrine actions on neurons (44, 45), and, by feeding back upon itself, low levels of this cytokine may be enough to drive potent neuroinflammatory changes in the brain. Also, IL-1R1 knockout mice presented a dramatic reduction in microglial and astrocytic activation as well as IL-6 and COX-2 production (45, 46). Adding to this evidence, overexpression of TOM1 suppressed the activation of the transcription factors nuclear factor- $\kappa$ B and activator protein 1 in response to IL-1 $\beta$  or TNF- $\alpha$  (47), and knockdown of TOM1 also resulted in the accumulation of IL-1R1 at late-stage endosomes (25).

Microglia are responsible for engulfing and degrading different types of brain cargo such as apoptotic cells and protein deposits (48), and the imbalance between protein production and degradation contributes to the characteristic extracellular accumulation of A $\beta$  in AD brains. Oligomeric A $\beta$  can activate microglia cells to induce neuroinflammation through processing of IL-1 $\beta$ , enhancing microglial neurotoxicity (49). Accordingly, infusion of human A $\beta$  in mice lacking the IL-1 receptor antagonist induced microglial activation and pronounced loss of synaptic markers (50). Here, knocking down TOM1 led to a reduced microglial branching and processes length and p62 levels, resulting in increased plaque load as well as A $\beta$  levels. More importantly, increasing TOM1 levels in microglia significantly augmented the rate of ADDLs and A $\beta$  fibrils phagocytosis, suggesting that the TOM1/IL-1R1 complex may play an additional role in the glial response to amyloid uptake (i.e., phagocytosis). A distinct phagocytic response of microglial cells to both A $\beta$  oligomers and fibrils has been shown, whereas exposure of microglia to fibrils enhanced phagocytosis (51), which could also explain the faster rate at which we observed fibril phagocytosis in

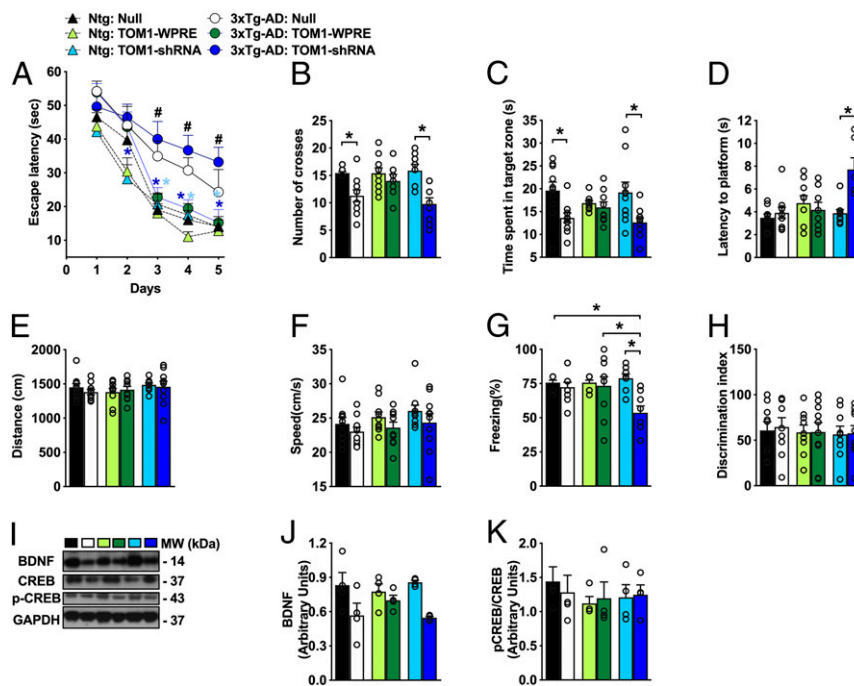


**Fig. 6.** Overexpression of TOM1 improves cognition. Knocking down TOM1 worsened the cognition of 3xTg-AD mice in the acquisition of the Morris water maze test (A). TOM1-shRNA also reduced the time spent in the target zone (B) and the number of crosses (C), while increasing the latency to platform (D). No significant changes were observed in distance (E) or speed (F) (a single asterisk represents significance vs. nTg group and “#” represents significance vs. TOM1-WPRE groups). TOM1-shRNA also reduced the freezing behavior in the contextual fear-conditioning paradigm (G). No significant changes were observed for the discrimination index during novel object recognition test (H). Representative Western blots and quantification show no significant changes in BDNF or pCREB/CREB ratio in all 3xTg-AD groups (I–K). Data are represented as mean ± SEM. ANOVA, \* $P \leq 0.05$ ;  $n = 4–10$  per group.

our study. Interestingly, increasing TOM1 levels exacerbated the internalization of ADDLs, an important finding, as A $\beta$  oligomers are considered the most deleterious form of this peptide.

The specialized process of protein internalization requires the ubiquitylation of cargo proteins and endocytosis, as well as protein-sorting complexes, followed by cargo delivery into early endosomes (52). Once internalized, cargo is further sorted through late endosomes and delivered for degradation in lysosomes. The endosomal signaling depends on the presence of highly specialized adaptor proteins, such as the TOM1 family (53, 54). TOM1 interacts with clathrin, implying its role in membrane trafficking (54), and the TOM1/Tollip association inhibits binding of Tollip to phosphatidylinositol 3-phosphate, facilitating its involvement in the TOM1-mediated endosomal cargo trafficking (27). TOM1 levels are reduced in AD brains (35, 55, 56) and, given the important body of evidence recently indicating that disturbed vesicular trafficking has a special relevance in AD pathogenesis (29, 31, 57, 58), the modulation of endocytosis and signaling may provide an effective means of regulating IL-1 $\beta$ -triggered inflammation in AD.

The initial amyloidogenic processing of APP by BACE1 occurs in the early endosomes (59). Additionally, the enlarged endosomes that are present in the early stages of AD (60) could be a result of abnormal internalization of BACE1 and APP, resulting in increased A $\beta$  production. The rapid trafficking of BACE1 to recycling endosomes, coupled with reduced levels of APP and A $\beta$  production, is mediated by GGA1 (61). GGAs (Golgi-localizing,  $\gamma$ -adaptin ear domain homology, ARF-binding proteins) are a family of monomeric adaptor proteins that regulate clathrin-mediated trafficking to endosomes. The GGA molecule is composed of four distinct domains, being the TOM1 part of the GAT domain (62). It has been recently shown that TOM1 attenuated the neuronal accumulation of A $\beta$  through binding to the Fc $\gamma$ -receptor IIb (Fc $\gamma$ RIIb) in male 3xTg-AD mice (63). In our study, overexpression of TOM1 resulted in reduced levels of

BACE1 in 3xTg-AD mice, suggesting that the dysregulation of BACE1 internalization might be a fundamental mechanism in the increased plaque formation observed.

Importantly, our data underscore an important mechanism through which IL-1 $\beta$  and IL-1R1 are related to A $\beta$  accumulation. Our results demonstrate that changes in TOM1-mediated endocytosis are A $\beta$ -triggered events leading to exacerbated inflammatory response and cognitive decline. Thus, embracing the restoration of TOM1-controlled inflammatory pathways therapeutically represents a promising strategy for the restoration of the aged immune system, which might prove effective for a healthy aging and control of age-dependent chronic neurodegenerative disorders.

## Methods

**Transgenic Mice.** All experiments were conducted with female homozygous 3xTg-AD and nTg mice aged 12 mo on a hybrid 129/C57BL6 background. The generation and characterization of the 3xTg-AD mice has been previously described (16). All animal procedures were performed in accordance with National Institutes of Health and University of California guidelines and were approved by the Institutional Animal Care and Use Committee at the University of California, Irvine.

**Human Tissue.** The University of California Irvine Alzheimer’s Disease Research Center provided the samples of human hippocampus from nondemented and AD subjects (SI Appendix, Table S1). The protocols for obtaining post-mortem brain tissue complied with all federal and institutional guidelines with special respect for donor identity confidentiality and informed consent.

**Infusion of Vectors.** Stereotaxic injection of AAV1-Null, AAV1-CAG-mTom1-WPRE, AAV1-GFP-U6-mTom1-shRNA, and AAV1-GFP-U6-mTollip-shRNA into the hippocampus was performed according to previously described surgical protocols (64). Female 9-mo-old 3xTg-AD mice were anesthetized and placed in stereotaxic apparatus under continuous isoflurane anesthesia. Two microliters of each AAV ( $1 \times 10^{10}$  genome particles/mL, Vector Biolabs) were injected at the following stereotaxic coordinates—anterior–posterior:  $-2.06$  mm; dorsoventral:  $-1.95$  mm; and mediolateral:  $\pm 1.75$  mm. Animals were allowed to

recover on a heating pad before being placed back in their home cages. Behavioral experiments and brain collection were performed 3 mo after the infusion of vectors.

#### Lentiviral Transduction and ADDLs Treatment in iPSC-Derived Human Microglia Cells.

iPSC microglia were differentiated according to previously published protocols (65). iPSC microglia were preincubated with 6  $\mu\text{g}/\text{mL}$  polybrene for 1 h. Lentiviral particles [Lenti ORF particles, TOM1 (Myc-DDK-tagged)-Human target of myb1 (chicken) (TOM1), transcript variant 1, and Lenti ORF control particles of pLenti-C-Myc-DDK-P2A-Puro, OriGene] were resuspended in fresh medium supplemented with 6  $\mu\text{g}/\text{mL}$  polybrene at  $1.25 \times 10^6$  transduction units per milliliter. Viral particles were added to Matrigel-coated plates and covered with 1 million iPSC microglia (MOI 1.25). Fresh medium was added for the next 2 d, and cells were harvested 3 d post transduction. Mature iPSC microglia were treated with 100 or 500 nM ADDL or vehicle for 24 or 48 h. ADDLs and fluorescent-tagged ADDLs (Anaspec HiLyte555) were prepared as previously described protocols (66). ADDL concentration was determined by Nanodrop (ThermoFisher Scientific) and fluorescent-tagged ADDL concentration was determined by interpolating to a standard curve of a 555-tagged protein (goat anti-mouse Alexa 555). For fibrils, fluorescent A $\beta$  was resuspended in 0.1%  $\text{NH}_4\text{OH}$ , diluted to 100  $\mu\text{g}/\text{mL}$  in sterile RNase/DNase free  $\text{H}_2\text{O}$ , and allowed to fibrillize for 1 wk at 37 C before use. At collection, iPSC microglia were washed with ice-cold Dulbecco's phosphate-buffered saline and lysed in SDS buffer (1% SDS, 1 mM  $\text{Na}_3\text{VO}_4$ , 10 mM Tris-HCl [pH 7.4]) with 20 $\times$  trituration.

**Real-Time Phagocytosis Assay.** Mature iPSC microglia were plated on Matrigel (Corning) at 40% confluence and allowed to settle for 20 min. Next, A $\beta$  preparations were added at the indicated concentrations and imaged hourly on the Essen S3 IncuCyte (Essen Biosciences) live-cell imaging platform. After image acquisition, masks of phase and fluorescent signal were generated with IncuCyte analysis software. Fluorescent signal was normalized to phase confluence to generate percentage of phagocytosis.

**Behavior Paradigms.** Behavioral analyses were done 3 mo after the infusion of vectors.

**Novel object.** Each mouse was habituated to an empty Plexiglas arena (45  $\times$  25  $\times$  20 cm) for 4 consecutive days prior to testing. The lighting intensity in each behavioral task was measured at 44 lx. Mice were exposed to 2 identical objects placed at opposite ends of the arena for 10 min. After 24 h, mice were presented for 10 min with one of the familiar and a novel object of similar dimensions. The discrimination index represents the percentage of time that mice spent exploring the novel object (67).

**Morris water maze.** Mice were trained to swim to a 14-cm diameter circular clear Plexiglas platform submerged 1.5 cm beneath the surface. Four trials were performed per day, for 60 s each with a 5-min interval between trials. The probe test was assessed 24 h after the last trial, with the platform removed. Performance was monitored with the EthoVision XT video-tracking system (Noldus Information Technology).

**Contextual fear conditioning.** During training, mice were placed in the fear-conditioning chamber and allowed to explore for 2 min before receiving 3 electric foot shocks (duration: 1 s; intensity: 0.2 mA; inter-shock interval: 2 min).

Twenty-four hours later, behavior in the conditioning chamber was observed and analyzed for freezing behavior during 5 min.

**Imaris Quantitative Analysis.** Volumetric image measurements were made in the hippocampus using Imaris software (Bitplane Inc.). Amyloid burden was acquired by measuring the total number of A $\beta$  plaques and their size, expressed in area units ( $\mu\text{m}^2$ ) in the whole hippocampal area analyzed. The 6E10-immunopositive signal (A $\beta$  plaques) within the selected brain region was identified by a threshold level mask, which was maintained throughout the whole analysis for uniformity. The total number of amyloid plaques and their area was obtained automatically by Imaris software. Quantitative comparisons between groups were always carried out on comparable sections of each animal processed at the same time with the same batches of solutions. Microglial and astroglial loading were defined as the percentage of area stained with anti-Iba1/anti-GFAP related to the hippocampal area analyzed (CA1 + subiculum). The Iba1/GFAP-immunopositive signal within the selected brain region was again identified by a threshold level mask (maintained throughout the whole analysis). All parameters analyzed were obtained with the Bitplane Imaris software.

**Electron Microscopy Immunogold Labeling.** Electron microscopy labeling of IL-1R1 was performed as previously described (68). Coronal sections were first cryoprotected in a 25% sucrose and 10% glycerol solution, followed by freezing at  $-80^\circ\text{C}$  in order to increase the antibody binding efficiency. The tissue was then incubated with IL-1R1 primary antibody for 48 h at 22 C followed by the incubation with 1.4 nm of gold-conjugated secondary antibody (1:100, Nanoprobes) overnight at 22 C. After postfixing with 2% glutaraldehyde, the labeling was enhanced with the HQ SilverTM Kit (Nanoprobes), and gold-toned. Immunolabeled sections were fixed in osmium tetroxide, block-stained with uranyl acetate, dehydrated in graded acetone, and embedded in Araldite (EMS). Selected areas were cut in ultrathin sections (70 nm) and examined with an electron microscope (JEOL JEM 1400).

**Statistical Analysis.** All data were analyzed by Student's *t* test comparisons, between 2 groups, and 1- or 2-way ANOVA, followed by Tukey's test for comparisons among more than 2 groups using Prism version 6.0 (GraphPad Software). *P* < 0.05 was considered significant, and the significance was set at 95% of confidence. Western blots, immunostainings, and cell culture analyses were repeated 3 to 4 times with similar results. Electrochemiluminescence-linked immunoassays were performed in duplicates. All values are presented as mean  $\pm$  SEM.

**ACKNOWLEDGMENTS.** This study was supported by the Larry L. Hillblom Foundation Grants 2016-A-016-FEL (to A.C.M.) and 2013-A-016-FEL (to D.B.-V.); the Alzheimer's Association Grants AARF-16-440760 (to S.F.) and NIRG-15-363477 (to D.B.-V.); NIH Grants NIH/NIA AG00538, AG054884, AG16573, AG027544 (to F.M.L.), ES024331 (to M.K.), and AG048099, AG055524, AG056303 (to M.B.-J.); Training Grant NS082174 (to A.M.), BrightFocus Foundation Grant A20155355 (to F.M.L.); Instituto de Salud Carlos III of Spain, cofinanced by European Regional Development Fund funds from the European Union Grants FIS P115/00796 and P118/01557 (to A.G.); and the Australian National Health and Medical Research Council Grants GNT112919, GNT1128436, and GNT1139469 (to R.M.). We thank Professor Giles Alexander Rae for his diligent proofreading of this manuscript.

1. A. C. Shaw, D. R. Goldstein, R. R. Montgomery, Age-dependent dysregulation of innate immunity. *Nat. Rev. Immunol.* **13**, 875–887 (2013).
2. H. H. Arnardottir, J. Dallj, R. A. Colas, M. Shinohara, C. N. Serhan, Aging delays resolution of acute inflammation in mice: Reprogramming the host response with novel nano-proresolving medicines. *J. Immunol.* **193**, 4235–4244 (2014).
3. C. Franceschi, P. Garagnani, P. Parini, C. Giuliani, A. Santoro, Inflammaging: A new immunometabolic viewpoint for age-related diseases. *Nat. Rev. Endocrinol.* **14**, 576–590 (2018).
4. E. A. Newcombe *et al.*, Inflammation: The link between comorbidities, genetics, and Alzheimer's disease. *J. Neuroinflammation* **15**, 276 (2018).
5. Q. Li, N. Y. Spencer, N. J. Pantazis, J. F. Engelhardt, Alsin and SOD1(G93A) proteins regulate endosomal reactive oxygen species production by glial cells and proinflammatory pathways responsible for neurotoxicity. *J. Biol. Chem.* **286**, 40151–40162 (2011).
6. J. Neefjes, R. van der Kant, Stuck in traffic: An emerging theme in diseases of the nervous system. *Trends Neurosci.* **37**, 66–76 (2014).
7. L. Li, N. Soetandyo, Q. Wang, Y. Ye, The zinc finger protein A20 targets TRAF2 to the lysosomes for degradation. *Biochim. Biophys. Acta* **1793**, 346–353 (2009).
8. F. Dodeller, M. Gottar, D. Huesken, V. Iourgenko, B. Cenni, The lysosomal transmembrane protein 9B regulates the activity of inflammatory signaling pathways. *J. Biol. Chem.* **283**, 21487–21494 (2008).
9. J. Cendrowski, A. Mamińska, M. Miaczynska, Endocytic regulation of cytokine receptor signaling. *Cytokine Growth Factor Rev.* **32**, 63–73 (2016).
10. M. Kitazawa, S. Oddo, T. R. Yamasaki, K. N. Green, F. M. LaFerla, Lipopolysaccharide-induced inflammation exacerbates tau pathology by a cyclin-dependent kinase 5-mediated pathway in a transgenic model of Alzheimer's disease. *J. Neurosci.* **25**, 8843–8853 (2005).
11. M. Kitazawa *et al.*, Blocking IL-1 signaling rescues cognition, attenuates tau pathology, and restores neuronal  $\beta$ -catenin pathway function in an Alzheimer's disease model. *J. Immunol.* **187**, 6539–6549 (2011).
12. F. L. Sciacca *et al.*, Interleukin-1B polymorphism is associated with age at onset of Alzheimer's disease. *Neurobiol. Aging* **24**, 927–931 (2003).
13. F. Licastro *et al.*, Increased plasma levels of interleukin-1, interleukin-6 and alpha-1-antichymotrypsin in patients with Alzheimer's disease: Peripheral inflammation or signals from the brain? *J. Neuroimmunol.* **103**, 97–102 (2000).
14. Y. Li, L. Liu, S. W. Barger, W. S. Griffin, Interleukin-1 mediates pathological effects of microglia on tau phosphorylation and on synaptophysin synthesis in cortical neurons through a p38-MAPK pathway. *J. Neurosci.* **23**, 1605–1611 (2003).
15. A. Mishra, H. J. Kim, A. H. Shin, S. A. Thayer, Synapse loss induced by interleukin-1 $\beta$  requires pre- and post-synaptic mechanisms. *J. Neuroimmune Pharmacol.* **7**, 571–578 (2012).
16. S. Oddo *et al.*, Triple-transgenic model of Alzheimer's disease with plaques and tangles: Intracellular A $\beta$  and synaptic dysfunction. *Neuron* **39**, 409–421 (2003).
17. A. M. Hein *et al.*, Sustained hippocampal IL-1 $\beta$  overexpression impairs contextual and spatial memory in transgenic mice. *Brain Behav. Immun.* **24**, 243–253 (2010).
18. G. A. Prieto *et al.*, Synapse-specific IL-1 receptor subunit reconfiguration augments vulnerability to IL-1 $\beta$  in the aged hippocampus. *Proc. Natl. Acad. Sci. U.S.A.* **112**, E5078–E5087 (2015).

19. B. P. Curran, H. J. Murray, J. J. O'Connor, A role for c-Jun N-terminal kinase in the inhibition of long-term potentiation by interleukin-1beta and long-term depression in the rat dentate gyrus *in vitro*. *Neuroscience* **118**, 347–357 (2003).
20. A. Kelly *et al.*, Activation of p38 plays a pivotal role in the inhibitory effect of lipopolysaccharide and interleukin-1 beta on long term potentiation in rat dentate gyrus. *J. Biol. Chem.* **278**, 19453–19462 (2003).
21. Y. Huang, D. E. Smith, O. Ibáñez-Sandoval, J. E. Sims, W. J. Friedman, Neuron-specific effects of interleukin-1 $\beta$  are mediated by a novel isoform of the IL-1 receptor accessory protein. *J. Neurosci.* **31**, 18048–18059 (2011).
22. S. L. Patterson, Immune dysregulation and cognitive vulnerability in the aging brain: Interactions of microglia, IL-1beta, BDNF and synaptic plasticity. *Neuropharmacology* **96**, 11–18 (2015).
23. K. Burns *et al.*, Tollip, a new component of the IL-1RI pathway, links IRAK to the IL-1 receptor. *Nat. Cell Biol.* **2**, 346–351 (2000).
24. A. Didierlaurent *et al.*, Tollip regulates proinflammatory responses to interleukin-1 and lipopolysaccharide. *Mol. Cell. Biol.* **26**, 735–742 (2006).
25. B. Brissoni *et al.*, Intracellular trafficking of interleukin-1 receptor I requires Tollip. *Curr. Biol.* **16**, 2265–2270 (2006).
26. E. E. Qvarnstrom, R. C. Page, S. Gillis, S. K. Dower, Binding, internalization, and intracellular localization of interleukin-1 beta in human diploid fibroblasts. *J. Biol. Chem.* **263**, 8261–8269 (1988).
27. S. Xiao *et al.*, Tom1 modulates binding of tollip to phosphatidylinositol 3-phosphate via a coupled folding and binding mechanism. *Structure* **23**, 1910–1920 (2015).
28. T. Wang, N. S. Liu, L. F. Seet, W. Hong, The emerging role of VHS domain-containing Tom1, Tom1L1 and Tom1L2 in membrane trafficking. *Traffic* **11**, 1119–1128 (2010).
29. S. Gao, A. E. Casey, T. J. Sargeant, V. P. Mäkinen, Genetic variation within endolysosomal system is associated with late-onset Alzheimer's disease. *Brain* **141**, 2711–2720 (2018).
30. R. S. Omri *et al.*, Differential effects of Alzheimer's disease A $\beta$ 40 and 42 on endocytosis and intraneuronal trafficking. *Neuroscience* **373**, 159–168 (2018).
31. A. M. Miranda *et al.*, Neuronal lysosomal dysfunction releases exosomes harboring APP C-terminal fragments and unique lipid signatures. *Nat. Commun.* **9**, 291 (2018).
32. R. A. French *et al.*, Expression and localization of p80 and p68 interleukin-1 receptor proteins in the brain of adult mice. *J. Neuroimmunol.* **93**, 194–202 (1999).
33. E. Pinteaux, L. C. Parker, N. J. Rothwell, G. N. Luheshi, Expression of interleukin-1 receptors and their role in interleukin-1 actions in murine microglial cells. *J. Neurochem.* **83**, 754–763 (2002).
34. S. Alves *et al.*, Interleukin-2 improves amyloid pathology, synaptic failure and memory in Alzheimer's disease mice. *Brain* **140**, 826–842 (2017).
35. K. Makioka *et al.*, Immunolocalization of Tom1 in relation to protein degradation systems in Alzheimer's disease. *J. Neurol. Sci.* **365**, 101–107 (2016).
36. N. Myeku, M. E. Figueiredo-Pereira, Dynamics of the degradation of ubiquitinated proteins by proteasomes and autophagy: Association with sequestosome 1/p62. *J. Biol. Chem.* **286**, 22426–22440 (2011).
37. J. R. Babu, T. Geetha, M. W. Wooten, Sequestosome 1/p62 shuttles polyubiquitinated tau for proteasomal degradation. *J. Neurochem.* **94**, 192–203 (2005).
38. A. Caccamo, E. Ferreira, C. Branca, S. Oddo, p62 improves AD-like pathology by increasing autophagy. *Mol. Psychiatry* **22**, 865–873 (2017).
39. S. Ortega-Martinez, A new perspective on the role of the CREB family of transcription factors in memory consolidation via adult hippocampal neurogenesis. *Front. Mol. Neurosci.* **8**, 46 (2015).
40. J. S. Mu, W. P. Li, Z. B. Yao, X. F. Zhou, Deprivation of endogenous brain-derived neurotrophic factor results in impairment of spatial learning and memory in adult rats. *Brain Res.* **835**, 259–265 (1999).
41. F. Cirulli, A. Berry, F. Chiarotti, E. Alleva, Intrahippocampal administration of BDNF in adult rats affects short-term behavioral plasticity in the Morris water maze and performance in the elevated plus-maze. *Hippocampus* **14**, 802–807 (2004).
42. K. D. Mayer-Barber, B. Yan, Clash of the cytokine titans: Counter-regulation of interleukin-1 and type I interferon-mediated inflammatory responses. *Cell. Mol. Immunol.* **14**, 22–35 (2017).
43. M. G. Netea *et al.*, IL-1beta processing in host defense: Beyond the inflammasomes. *PLoS Pathog.* **6**, e1000661 (2010).
44. R. M. Gibson, N. J. Rothwell, R. A. Le Feuvre, CNS injury: The role of the cytokine IL-1. *Vet. J.* **168**, 230–237 (2004).
45. A. Depino, C. Ferrari, M. C. Pott Godoy, R. Tarelli, F. J. Pitossi, Differential effects of interleukin-1beta on neurotoxicity, cytokine induction and glial reaction in specific brain regions. *J. Neuroimmunol.* **168**, 96–110 (2005).
46. S. S. Shafteel *et al.*, Sustained hippocampal IL-1 beta overexpression mediates chronic neuroinflammation and ameliorates Alzheimer plaque pathology. *J. Clin. Invest.* **117**, 1595–1604 (2007).
47. M. Yamakami, H. Yokosawa, Tom1 (target of Myb 1) is a novel negative regulator of interleukin-1- and tumor necrosis factor-induced signaling pathways. *Biol. Pharm. Bull.* **27**, 564–566 (2004).
48. A. Sierra, O. Abiega, A. Shahraz, H. Neumann, Janus-faced microglia: Beneficial and detrimental consequences of microglial phagocytosis. *Front. Cell. Neurosci.* **7**, 6 (2013).
49. B. Parajuli *et al.*, Oligomeric amyloid  $\beta$  induces IL-1 $\beta$  processing via production of ROS: Implication in Alzheimer's disease. *Cell Death Dis.* **4**, e975 (2013).
50. J. M. Craft, D. M. Watterson, E. Hirsch, L. J. Van Eldik, Interleukin 1 receptor antagonist knockout mice show enhanced microglial activation and neuronal damage induced by intracerebroventricular infusion of human beta-amyloid. *J. Neuroinflammation* **2**, 15 (2005).
51. X. D. Pan *et al.*, Microglial phagocytosis induced by fibrillar  $\beta$ -amyloid is attenuated by oligomeric  $\beta$ -amyloid: Implications for Alzheimer's disease. *Mol. Neurodegener.* **6**, 45 (2011).
52. H. W. Platta, H. Stenmark, Endocytosis and signaling. *Curr. Opin. Cell Biol.* **23**, 393–403 (2011).
53. Y. Katoh *et al.*, Tollip and Tom1 form a complex and recruit ubiquitin-conjugated proteins onto early endosomes. *J. Biol. Chem.* **279**, 24435–24443 (2004).
54. M. Yamakami, T. Yoshimori, H. Yokosawa, Tom1, a VHS domain-containing protein, interacts with tollip, ubiquitin, and clathrin. *J. Biol. Chem.* **278**, 52865–52872 (2003).
55. A. Plaza-Zabala, V. Sierra-Torre, A. Sierra, Autophagy and microglia: Novel partners in neurodegeneration and aging. *Int. J. Mol. Sci.* **18**, E598 (2017).
56. A. François *et al.*, Involvement of interleukin-1 $\beta$  in the autophagic process of microglia: Relevance to Alzheimer's disease. *J. Neuroinflammation* **10**, 151 (2013).
57. L. S. Whyte, A. A. Lau, K. M. Hemsley, J. J. Hopwood, T. J. Sargeant, Endo-lysosomal and autophagic dysfunction: A driving factor in Alzheimer's disease? *J. Neurochem.* **140**, 703–717 (2017).
58. E. Schmukler, D. M. Michaelson, R. Pinkas-Kramarski, The interplay between apolipoprotein E4 and the autophagic-endocytic-lysosomal axis. *Mol. Neurobiol.* **55**, 6863–6880 (2018).
59. E. H. Koo, S. L. Squazzo, Evidence that production and release of amyloid beta-protein involves the endocytic pathway. *J. Biol. Chem.* **269**, 17386–17389 (1994).
60. R. A. Nixon, Endosome function and dysfunction in Alzheimer's disease and other neurodegenerative diseases. *Neurobiol. Aging* **26**, 373–382 (2005).
61. W. H. Toh, P. Z. C. Chia, M. I. Hossain, P. A. Gleeson, GGA1 regulates signal-dependent sorting of BACE1 to recycling endosomes, which moderates A $\beta$  production. *Mol. Biol. Cell* **29**, 191–208 (2018).
62. Y. Shiba *et al.*, GAT (GGA and Tom1) domain responsible for ubiquitin binding and ubiquitination. *J. Biol. Chem.* **279**, 7105–7111 (2004).
63. Y. Gwon *et al.*, TOM1 regulates neuronal accumulation of amyloid- $\beta$  oligomers by Fc $\gamma$ RIIb2 variant in Alzheimer's disease. *J. Neurosci.* **38**, 9001–9018 (2018).
64. M. Blurton-Jones *et al.*, Neural stem cells improve cognition via BDNF in a transgenic model of Alzheimer disease. *Proc. Natl. Acad. Sci. U.S.A.* **106**, 13594–13599 (2009).
65. A. McQuade *et al.*, Development and validation of a simplified method to generate human microglia from pluripotent stem cells. *Mol. Neurodegener.* **13**, 67 (2018).
66. W. L. Klein, Abeta toxicity in Alzheimer's disease: Globular oligomers (ADDLs) as new vaccine and drug targets. *Neurochem. Int.* **41**, 345–352 (2002).
67. D. Baglietto-Vargas, R. Medeiros, H. Martinez-Coria, F. M. LaFerla, K. N. Green, Mifepristone alters amyloid precursor protein processing to preclude amyloid beta and also reduces tau pathology. *Biol. Psychiatry* **74**, 357–366 (2013).
68. A. Gomez-Arboledas *et al.*, Phagocytic clearance of presynaptic dystrophies by reactive astrocytes in Alzheimer's disease. *Glia* **66**, 637–653 (2018).